Road Cycling Climbs Made Speedier by Personalized Pacing Strategies

Stefan Wolf[1], Raphael Bertschinger[2] and Dietmar Saupe[1]
[1]*Department of Computer and Information Science, University of Konstanz, Konstanz, Germany*
[2]*Department of Sports Science, University of Konstanz, Konstanz, Germany*
{*s.wolf, raphael.bertschinger, dietmar.saupe*}*@uni-konstanz.de*

Keywords: Optimal Strategies, Critical Power, Road Cycling, Optimal Feedback

Abstract: Lately, modeling and optimizing endurance performance has become popular. Optimal strategies have been calculated for running as well as for cycling. Since most of these studies are of theoretical nature, we performed a series of experiments to determine whether race performance can actually be improved using mathematical optimization in a realistic scenario. The optimal strategy was based on the equations of motion for cycling and an individual critical power model for each rider. Constant visual feedback based on the calculated strategy was given to the rider while performing a real world climb on a bike simulator in the laboratory. The aim of this study was to determine whether these strategies are feasible and effective. The results showed that feedback in general and the optimal strategy feedback in particular led to a significant improvement. The total race times decreased between 0.8% and 3.2% employing optimal strategy feedback compared to self paced rides.

1 INTRODUCTION

What makes a winner in endurance races like a Tour de France stage? Besides pre-race preparations, the strategy during the race has a major influence on victory or defeat. During recent years, optimizing pacing strategies based on mathematical models has become more and more popular. Mainly running and cycling individual time trials have been investigated.

First results for cycling were gathered by Gordon (2005). The 3-parameter critical power model of Morton (1996) and a simple mechanical model which includes air resistance, friction and gravitation were used to analytically calculate strategies on simple, piecewise constant courses.

An extension of this work has been provided by Dahmen et al. (2012). The more realistic mechanical model of Martin et al. (1998), which also includes inertia and bearing friction as well as slope profiles of real world courses has been used. Due to the higher complexity of the optimization problem, numerical methods were applied.

Since then several studies have been published that apply more sophisticated physiological models. For example, Sundström et al. (2014) compared strategies with the traditional critical power model to a more versatile 3-component model which was introduced by Morton (1986).

All of the current studies in this field are mainly of theoretical nature and it still remains to be shown whether one can improve realistic rides using optimized strategies. For this purpose, we present an experiment where a mathematically calculated, optimal strategy has been used to provide visual feedback during a simulated ride on a real world course in the laboratory.

We provide an experimental setting to answer whether the calculated optimal strategies are feasible i.e. the riders are able to follow the strategy until the end. Moreover, we determined the resulting improvement in performance. This study presents the underlying mathematical models, the parameter estimation process and the results.

2 METHODS

2.1 Experimental Setup

Six healthy male subjects (mean standard deviation; age = 27.7 ± 4.2 years; height = 182.6 ± 5.3 cm; weight = 76.3 ± 5.3 kg) participated in the study after giving informed consent. Aerobic capacity was heterogeneous throughout the group of subjects, indicated by the power to weight ratio at the blood lactate threshold (Table 1). Subjects were asked to refrain

from caffeine and alcohol at least one night and from intense physical activity at least two days prior the experiment.

All tests were performed on a bike simulator based on a Cyclus2 brake (RBM elektronik-automation GmbH, Germany) and a customized simulator software (Dahmen et al., 2011). Figure 1 shows the visual interface of the simulator which is projected on the wall in front of the rider.

Figure 1: Visual interface of the simulator. The top graph shows the slope profile and the position on the course. In the background a video of the track is played which is synchronized to the simulated speed. On the bottom current status information like traveled distance, speed or power output is shown. Best viewed electronically.

The experiment incorporated five tests with rest periods of one week between each test. At first, each subject performed an incremental step test to exhaustion starting at 100 W with increments of 20 W every 3 minutes to obtain an estimate of his anaerobic lactate threshold (AT). The other tests were simulated rides on a real course, namely the eastern climb of the Flüela Pass in Switzerland. More details about the course are provided below.

The first simulation ride (I) was for familiarization purposes. In order to obtain a suitable benchmark, subjects were advised to ride close to their AT but were free in the selection of their power output. In the second ride (II) subjects rode with their own pacing strategy. In rides I and II subjects were instructed to perform with maximal effort.

The third ride (III) was performed with an optimal strategy feedback and the fourth ride (IV) with a validation strategy feedback. The optimal strategy was obtained by solving the optimal control problem described below. Whereas the energy expenditure in the optimal strategy was similar to rides I and II, the race time was shorter than that achieved in those rides.

The validation strategy was determined by adding a constant power offset to the riders' own strategy of ride II in order to achieve the same time as with the optimal strategy. The individual power offsets are shown in Table 1. Obviously the energy demand in this ride was higher than in ride II and the intended race time was the same as in ride III.

Rides III and IV were performed in random order. Subjects 1, 3, 4 and 6 performed ride III first, subjects 2 and 5 performed ride IV first. The subjects were not told which strategies the feedback during rides III and IV was based on. In both rides the subjects got a continuous visual feedback of the gap to a virtual rider cycling with the proposed strategy. The feedback is shown in Figure 1 in the status information (third row from below). Colors changed from red (behind) to green (in range) to blue (in front). The subjects were advised to keep that gap as small as possible and stay in a range of $\pm$2m.

Table 1: Weight, height and power-to-weight ratio (PTW) at the lactate threshold of the six subjects and the power offsets ΔP between ride II and ride IV.

	weight (kg)	height (cm)	PTW (W/kg)	ΔP (W)
subject 1	83.1	192	4.6	3.6
subject 2	80.7	184	3.0	3.6
subject 3	72.5	182	4.6	4.6
subject 4	68.5	180	2.8	4.9
subject 5	76.2	182	3.7	6.1
subject 6	77.0	176	3.1	10.2

2.2 Course Overview

The eastern climb of the Flüela Pass in Switzerland starting in Susch (Figure 2) was choosen for all simulated rides. It has a length of around 12 km and a total climb of 923 m. The slope varies from 2.1 % to 11.8 % with a mean value of 8.1 %. An overview over the altitude and slope profiles is given in Figure 3.

Figure 2: Eastern climb of the Flüela pass in Switzerland starting in Susch. (©2016 Google, Image ©2016 DigitalGlobe).

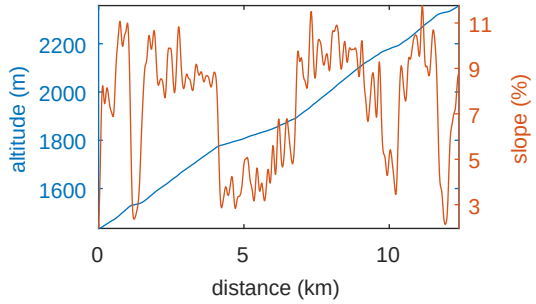

Figure 3: Altitude and slope profile of the course.

2.3 Mechanical Model

To model the relationship between the power output P of the rider and the resulting speed v the well known model of Martin et al. (1998) was used. It has been validated in (Dahmen et al., 2011) on real world courses as well as in a laboratory simulator setup.

The model is based on the equilibrium of the riders' pedal power P and the power induced by aerodynamic drag P_{air}, friction P_{roll}, gravitation P_{pot} and inertia P_{kin} as shown in Equation 1.

$$\eta P = \underbrace{mgsv}_{P_{\text{pot}}} + \underbrace{\mu mgv}_{P_{\text{roll}}} + \underbrace{\left(m + \frac{I_w}{r_w^2}\right)\dot{v}v}_{P_{\text{kin}}} + \underbrace{\frac{1}{2}c_d \rho A v^3}_{P_{\text{air}}} \quad (1)$$

An overview over the model parameters is given in Table 2. Since a steep uphill course was simulated, bearing resistances had an insignificant impact compared to P_{pot} and therefore were neglected.

Table 2: Parameters of the mechanical model as they were used in the simulator and the optimization.

parameters		
description	variable	value
cyclist mass	m_{rider}	Table 1
bike mass	m_{bike}	10 kg
total mass	m	$m_{\text{rider}} + m_{\text{bike}}$
gravity factor	g	$9.81\,\text{m/s}^2$
slope of the course	s	Figure 3
friction factor	μ	0.004
wheel inertia	I_w	$0.2\,\text{kgm}^2$
wheel radius	r_w	0.335 m
simulator inertia	I_s	$0.658\,\text{kgm}^2$
drag coefficient	c_d	0.7
air density	ρ	$1.2\,\text{kg/m}^3$
cross-sectional area	A	$0.4\,\text{m}^2$
chain efficiency	η	0.95

In the simulator we were not able to simulate inertia realistically, so the influence of inertia was reduced to the impact of the brake's flywheel. This depends on the fixed mechanical gear ratio (50/13) and the virtual gear ratio which was chosen by the rider during the experimental rides. Since a steep uphill course was simulated, riders were using the smallest available virtual gear ratio of 33/31 most of the time. Therefore, the contribution of kinetic energy to the model is given by Equation 2.

$$P_{\text{kin}} = \left(\frac{33}{32}\cdot\frac{13}{50}\right)^2 \frac{I_s}{r_w^2}\dot{v}v =: M\dot{v}v \quad (2)$$

where $M = \left(\frac{33}{32}\cdot\frac{13}{50}\right)^2 \frac{I_s}{r_w^2}$.

Another modification from the original model was done to achieve a better numerical stability in the optimization problem. In (Dahmen and Brosda, 2016) it was suggested to substitute the speed v by the kinetic energy $e_{\text{kin}} = \frac{1}{2}Mv^2$. Equation 3 shows the final model formula giving the kinetic energy dynamics $\dot{e}_{\text{kin}}$ based on a certain power output P.

$$\begin{aligned}\dot{e}_{\text{kin}} &= \eta P - \left(\frac{\rho c_w A}{M} e_{\text{kin}} + \mu mg + mgs(x)\right)\sqrt{\frac{2e_{\text{kin}}}{M}} \\ &=: F_{\text{mech}}(e_{\text{kin}}, x, P)\end{aligned} \quad (3)$$

2.4 Physiological Model

To simulate the athletes' energy expenditure throughout the race the critical power concept introduced by Monod and Scherrer (1965) was used. It models the relationship between a constant power output P and the corresponding time to exhaustion.

An abstract representation as a hydraulic model is given in Figure 4. Two energy resources were considered: the aerobic energy resource (O) which is unlimited in size but has a limited access rate called critical power (P_C) and the anaerobic energy resource (E_{an}) which is limited in size.

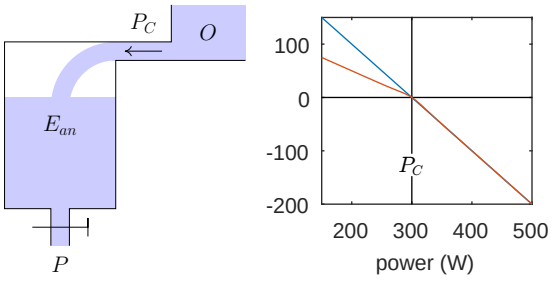

Figure 4: Flow model of the Critical Power model (left) and the rate of change in the anaerobic work capacity level for a certain power output (right). The blue curve shows the original critical power model while the red curve shows the modified version with $\alpha = 0.5$.

While the model originally was designed for constant work rate exercise, a dynamic version is derived easily from the hydraulic model. The change

$\dot{e}_{\text{an}}$ of the remaining amount of fluid in the anaerobic work capacity vessel is given by the difference of the amount of fluid flowing into the vessel (P_C) and the amount of fluid leaving the vessel (P), $P_C - P$.

First simulations indicated that the rate during recovery phases is too high in this classical model. Therefore we modified it by damping the recovery rate by a constant factor α. To get a smooth conjunction between recovery and exhaustion a tanh sigmoid function as shown in Equation 4 was used.

$$\begin{aligned}\dot{e}_{\text{an}} &= (P_C - P)\left(\frac{1-\alpha}{2}\tanh\left(-\frac{P_C - P}{20}\right) + \frac{1+\alpha}{2}\right) \\ &=: F_{\text{phys}}(P)\end{aligned} \tag{4}$$

Figure 4 shows the behavior of $\dot{e}_{\text{an}}$ for different power outputs.

2.4.1 Parameter Estimation

The three parameters P_C, E_{an} and α of the physiological model were determined with the step test and rides I and II by assuming that the athlete was completely recovered when the rides started and fully exhausted at the end of each test.

Therefore parameters were chosen in a way that the remaining anaerobic work capacity was zero at the end of the rides by minimizing its squared error as shown in Equation 5. To ensure that the remaining anaerobic work capacity e_{an} did not fall below zero and did not exceed the anaerobic work capacity vessels size E_{an} during the rides the boundary conditions in Equation 6 were added to the minimization problem.

$$\min \sum_{i=1}^{3} e_{\text{an},i}(T_i)^2 \tag{5}$$

$$0 \leq e_{\text{an},i}(t) \leq E_{\text{an}} \text{ for } i = 1,2,3 \text{ and } t \in [0, T_i] \tag{6}$$

$e_{\text{an},1}(t)$, $e_{\text{an},2}(t)$ and $e_{\text{an},3}(t)$ are the remaining anaerobic work capacities during the step test, ride I and ride II respectively and T_i are the corresponding test durations. The resulting parameters for each subject are shown in Table 3.

2.5 Optimal Control Problem

In order to calculate an optimal strategy the time T needed to complete a given course was minimized. To avoid singular problems a regularization variable Q was introduced. It is the derivative of the power P and the regularization discourages large power variations. This lead to the following optimal control problem.

Table 3: Physiological parameters of the subjects. The critical power P_C, the anaerobic work capacity E_{an} and the recovery damping factor α.

	P_C (W)	E_{an} (J)	α
subject 1	378	27465	0.10
subject 2	262	11999	0.49
subject 3	330	16432	0.63
subject 4	167	27038	0.16
subject 5	258	13789	0.20
subject 6	288	10616	0.11

Minimize the cost functional

$$J = T + \varepsilon \int_0^T Q(t)^2 dt$$

subject to the dynamic constraints

$$\begin{aligned}\dot{P}(t) &= Q(t) \\ \dot{x}(t) &= \sqrt{2e_{\text{kin}}(t)/M} \\ \dot{e}_{\text{kin}}(t) &= F_{\text{mech}}(e_{\text{kin}}(t), x(t), P(t)) \\ \dot{e}_{\text{an}}(t) &= F_{\text{phys}}(P(t))\end{aligned}$$

the path constraints

$$\begin{aligned}0 \leq\ & e_{\text{an}}(t) \leq\ E_{\text{an}} \\ 0 \leq\ & P(t) \leq\ P_m\end{aligned}$$

and the boundary conditions

$$\begin{aligned}x(0) &= 0 \\ x(T) &= x_f \\ e_{\text{kin}}(0) &= 0 \\ e_{\text{an}}(0) &= E_{\text{an}}\end{aligned}$$

where $P(t)$, $x(t)$, $e_{\text{kin}}(t)$ and $e_{\text{an}}(t)$ are the states, $Q(t)$ is the control, and x_f is the length of the course.

This problem was solved numerically by the state-of-the-art optimal control solver GPOPS-II (Patterson and Rao, 2014).

3 RESULTS

Figure 5 shows the strategy chosen by subject 1 in ride II as well as the calculated optimal strategy. Two main differences in the strategies can be observed: In the steep sections of the course the optimal strategy suggests a higher power output than the athlete chose whereas the athlete used this saved energy for a sprint in the end.

In general we observe that the optimal strategy is close to a constant power output with slightly higher values for steep segments and lower values for flat segments. Nearly all subjects chose a power output lower than the optimal one in the first 10 km and finished the ride with a sprint. Only subject 5 selected

Table 4: Total race-times for the self-paced rides II, rides III with optimal strategy feedback and the validation rides IV. There were no significant differences between the calculated optimal race-times and those of rides III. Additionally for rides III the improvement compared to rides II is provided in relative values as well as whether the subjects were able to follow the validation feedback in rides IV.

	ride II	ride III		ride IV	
	self-paced	optimal feedback		validation feedback	
	(hh:mm:ss)	(hh:mm:ss)	(%)	(hh:mm:ss)	(target time achieved)
subject 1	00:43:03	00:42:43	-0.77	00:42:43	yes
subject 2	01:00:12	00:59:26	-1.27	00:59:26	yes
subject 3	00:44:28	00:43:55	-1.24	00:44:44	no
subject 4	01:19:01	01:16:51	-2.74	01:18:42	no
subject 5	00:58:17	00:57:00	-2.20	00:57:49	no
subject 6	00:53:55	00:52:10	-3.24	00:52:10	yes

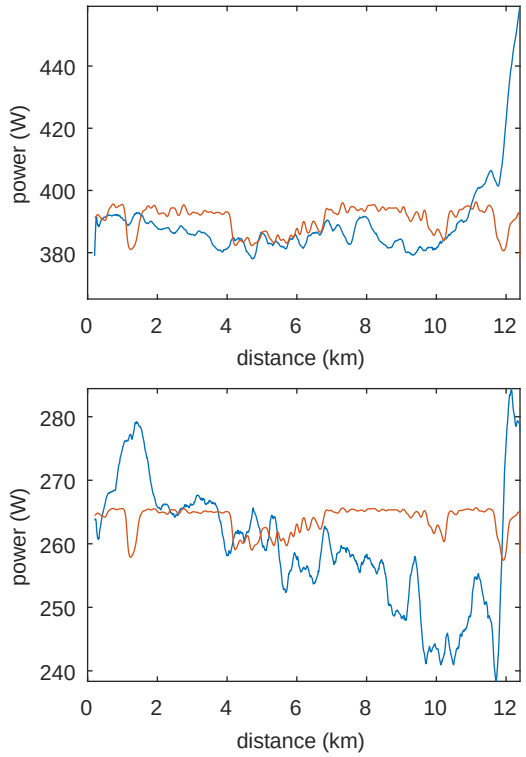

Figure 5: Power output for subject 1 (top) and subject 5 (bottom). The red curve is the calculated optimal power output and the blue curve is the power output during ride II smoothed with a Gaussian filter ($\sigma = 150$ m).

a different strategy by starting with a high power output, decreasing it during the ride and finishing with a sprint (Figure 5).

In the ride with optimal strategy feedback, all subjects were able to maintain the proposed strategy and finish with the time the optimal strategy predicted. This resulted in a reduction of the total race time compared to the self-paced ride II (Table 4). The relative improvement was between 0.8 % and 3.2 % corresponding to time savings between 20 s and 130 s.

Three out of six subjects (1, 2 and 6) were able to follow the validation strategy feedback and thus exactly achieved the target finishing time identical to that for the optimal pacing strategy. The other three riders (3, 4 and 5) failed in that regard, becoming too exhausted to maintain the proposed power output in the end of the ride. In Figure 6 this behavior is shown for subject 4. Until 10 km the subject was able to perform constantly above ride II but after that the performance dropped considerable.

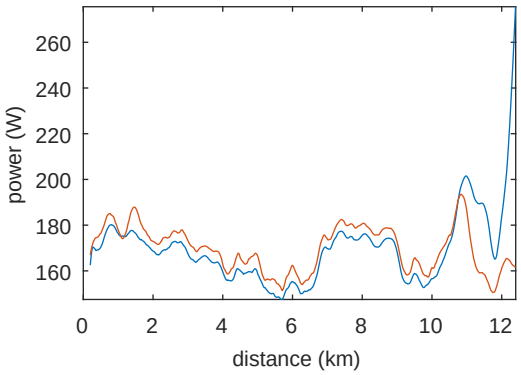

Figure 6: Power output for subject 4. The red curve is the power output during ride IV and the blue curve is the power output during ride II. Both are smoothed with a Gaussian filter ($\sigma = 150$ m).

4 DISCUSSION

In this study we addressed three questions:

1. Is it even possible to maintain the proposed optimal strategy?
2. Does the race time improve using optimal strategy feedback?

3. If so, does the race time improve because of the strategy or because of the fact that there is a pace maker?

The first two questions can be answered positively. All subjects were able to follow the optimal strategy until the end and the total race times improved for all subjects compared to their own paced rides.

To answer the third question the subjects performed ride IV. The feedback in ride IV implied a power output constantly above the power output of ride II. Since ride II was until exhaustion, it should have not been possible to maintain the proposed power output until the end of the ride.

Three out of six subjects confirmed this assumption. They were not able to follow the feedback given in ride IV in the last part of the race. Nevertheless the other three subjects were able to maintain the strategy until the end. This indicates that the feedback itself motivated them to access more energy resources than in their self paced ride.

Therefore question three cannot be answered clearly. Feedback alone enabled most subjects to improve their race times, even if they were not able to follow it until the end. But the three subjects that could not follow the feedback in ride IV until the end clearly showed that there is a definite advantage using the optimal strategy.

In order to answer the third question satisfactorily and distinguish between improvements due to the strategy and improvements due to the pace maker, a larger set of participants would be needed to be able to apply statistical methods and provide an adequate quantitative justification.

5 CONCLUSIONS

Our experiment showed that the calculated optimal strategy is feasible in a way that all athletes were able to follow it until the end. Furthermore, it provides an advantage over the strategy the athletes chose on their own.

Even though external feedback itself already enabled most subjects to improve their performance, a well chosen strategy like the calculated optimal strategy is required to ensure that the athlete can finish the race properly and enhance the total race time.

The next step to get closer to real racing conditions is to perform a similar experiment in the field. Therefore a feedback device has to be developed, which incorporates a pace maker based on GPS measurements.

Another major challenge arising with field tests is to consider wind conditions along the track and to provide a corresponding real-time adaptation of the optimal strategy.

REFERENCES

Dahmen, T. and Brosda, F. (2016). Robust computation of minimum-time pacing strategies on realistic road cycling tracks. In *Sportinformatik 2016*, 11. Symposium der dvs-Sektion Sportinformatik, Magdeburg, Germany. accepted.

Dahmen, T., Byshko, R., Saupe, D., Röder, M., and Mantler, S. (2011). Validation of a model and a simulator for road cycling on real tracks. *Sports Engineering*, 14(2-4):95–110.

Dahmen, T., Wolf, S., and Saupe, D. (2012). Applications of mathematical models of road cycling. *IFAC Proceedings Volumes*, 45(2):804–809.

Gordon, S. (2005). Optimising distribution of power during a cycling time trial. *Sports Engineering*, 8(2):81–90.

Martin, J. C., Milliken, D. L., Cobb, J. E., McFadden, K. L., and Coggan, A. R. (1998). Validation of a mathematical model for road cycling power. *Journal of applied biomechanics*, 14:276–291.

Monod, H. and Scherrer, J. (1965). The work capacity of a synergic muscular group. *Ergonomics*, 8(3):329–338.

Morton, R. H. (1986). A three component model of human bioenergetics. *Journal of mathematical biology*, 24(4):451–466.

Morton, R. H. (1996). A 3-parameter critical power model. *Ergonomics*, 39(4):611–619.

Patterson, M. A. and Rao, A. V. (2014). Gpops-ii: A matlab software for solving multiple-phase optimal control problems using hp-adaptive gaussian quadrature collocation methods and sparse nonlinear programming. *ACM Transactions on Mathematical Software (TOMS)*, 41(1):1.

Sundström, D., Carlsson, P., and Tinnsten, M. (2014). Comparing bioenergetic models for the optimisation of pacing strategy in road cycling. *Sports Engineering*, 17(4):207–215.